ACS OMEGA

http://pubs.acs.org/journal/acsodf

Article

Measurement and Prediction of Isothermal Vapor−Liquid Equilibrium and Thermodynamic Properties of a Turpentine + Rosin System Using the COSMO-RS Model

Youqi Li, Xiaopeng Chen, Linlin Wang, Xiaojie Wei, Minting Nong, Weijian Nong, and Jiezhen Liang*

Cite This: *ACS Omega* 2022, 7, 16270−16277

Read Online

ACCESS | Metrics & More | Article Recommendations

ABSTRACT: The vapor−liquid equilibrium (VLE) of components of a turpentine + rosin system were measured at 313.2 and 333.2 K using headspace gas chromatography. The thermodynamic properties of the turpentine + rosin system such as activity coefficients, total pressure, partial pressure, excess Gibbs energies, and excess enthalpies were calculated using the COSMO-RS model. The results showed that the activity coefficients were greater than 1 for all components of turpentine except for longifolene, indicating a positive deviation from Raoult's law for all components of turpentine except for longifolene. The total pressures were about 1 kPa at 313.2 K and about 3 kPa at 333.2 K. Meanwhile, the excess Gibbs energies G^E and excess enthalpies H^E of the system were positive, indicating that the mixing of the components of turpentine and rosin was endothermic. Moreover, the hydrogen bonding interaction energy H^E(hydrogen bonding) contributed the most for the excess enthalpies H^E.

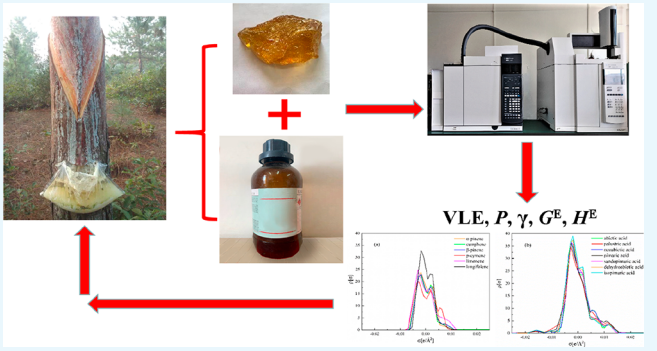

1. INTRODUCTION

Pine oleoresin, a highly viscous resin secreted from the resinous tract of pine trees,[1] is composed of turpentine (mono- and sesquiterpenes) and rosin (diterpenes). Rosin is a nonvolatile solid mixture with a higher boiling point. The main components of rosin are resin acids.[2,3] Rosin is widely used in materials, chemicals, and chemical engineering because of its excellent properties such as anticorrosion, moisture resistance, insulation, adhesion, and emulsification.[4−8] Turpentine mainly consists of monoterpenes and sesquiterpenes. The main components of monoterpenes are α-pinene, camphene, β-pinene, limonene, and p-cymene, which are easily volatile; the main component of sesquiterpenes is longifolene. Turpentine is applied widely in the synthesis of various fine chemicals, such as spices, medicine, and additives.[9−13] Since these pine oleoresin derivatives have various applications in chemical industries, higher oleoresin yields are economically desirable.

Currently, pine oleoresin is often extracted by tapping living trees with the "debarking" (bark-peeling) method, in which bark removal is performed periodically, allowing pine oleoresin to be secreted and collected. However, pine oleoresin tapping is open-ended. As the easily volatile components of turpentine, such as α-pinene, camphene, β-pinene, limonene, and p-cymene, are constantly evaporating into the atmosphere, about half of the turpentine yield is lost. Would the components of rosin (such as abietic acid, palustric acid, neoabietic acid, pimaric acid, sandopimaric acid, dehydroabietic acid, and isopimaric acid) have any effect on the interaction between the components of turpentine (such as α-pinene, camphene, β-pinene, limonene, p-cymene, and longifolene) and thus affect their volatilization? Therefore, vapor−liquid equilibrium (VLE) data of components of turpentine and rosin is worth investigating.

To date, some VLE data of the aforementioned components of turpentine have already been reported. The isobaric VLE data of an α-pinene + β-pinene system was obtained by Wang et al.[14] Sun et al.[15] reported the vacuum VLE data of an α-pinene + β-pinene + p-cymene system at 53.5 and 80 kPa. Ruan et al.[16] provided the isobaric VLE data for a pinane + α-pinene + longifolene system. In their work, the activity coefficients of each component in each binary system were derived, and the excess Gibbs energy and excess enthalpy were obtained. Wu et al.[17] reported the isobaric VLE data of binary systems with camphene, (+)-3-carene, (−)-β-caryophyllene, p-

Received: September 17, 2021
Accepted: April 21, 2022
Published: May 4, 2022

https://doi.org/10.1021/acsomega.1c05167
ACS Omega 2022, 7, 16270−16277

cymene, and α-pinene at 101.33 kPa. They found calculated values by NRTL, Wilson, and UNIQUAC models that were in good agreement with the experimental VLE data. However, fewer reports providing VLE data of systems containing components of rosin were found. Since both turpentine and rosin contain many components which are not easily separated, VLE data for the turpentine + rosin system measured by the usual method of Ellis and Rose using a double-cycle equilibrium kettle seemed difficult. Therefore, the headspace gas chromatography (HSGC) method is used for the determination of VLE because this method has several advantages such as short VLE time, low dosage of reagents, and accurate temperature control.[18−21]

In this work, the isothermal VLE of components of the turpentine + rosin system were measured using the HSGC method at 313.2 and 333.2 K. The thermodynamic properties such as activity coefficients, total pressure, partial pressure, excess Gibbs energies, and excess enthalpies of the system were calculated by the COSMOtherm software based on the COSMO-RS model to provide more basic data for the turpentine + rosin system.

2. RESULTS AND DISCUSSION

2.1. Applicability of the COSMO-RS Model. In order to investigate the applicability of the COSMO-RS model to the system in this work, the isothermal VLE data of a β-pinene (1) + *p*-cymene (2) system in the literature[22] were selected and compared with the values calculated using the COSMO-RS

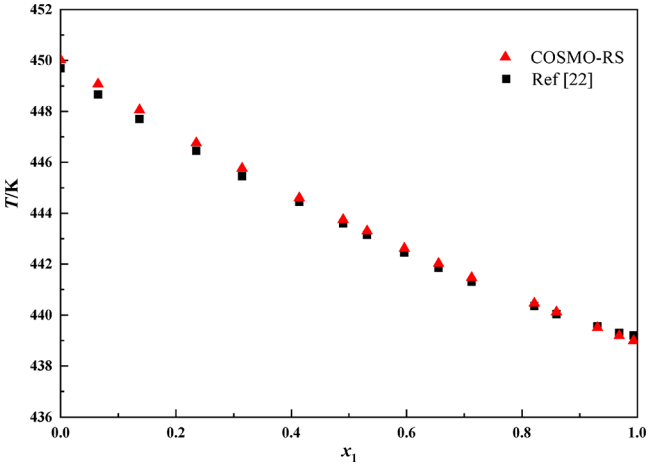

Figure 1. Comparison of calculated and literature data[22] for $T-x$ of the β-pinene (1) + *p*-cymene (2) system at 100.7 kPa.

model in this work, as shown in Figure 1. The average absolute percentage deviation (AAPD) was calculated by eq 1.

$$\mathrm{AAPD}(T_i) = \frac{\sum_{i=1}^{n} \frac{|T_{i,\cos} - T_{i,Ref}|}{T_{i,\cos}} \times 100\%}{n} \quad (1)$$

where $T_{i,\cos}$ is the temperature calculated by COSMO-RS and $T_{i,\mathrm{ref}}$ is the temperature from the literature.[22]

The obtained AAPD was 0.04%, indicating that the calculated data with the COSMO-RS model were in good agreement with the literature data. Thus, the COSMO-RS model can be applied to predict the VLE data for the turpentine + rosin system in this study.

2.2. Vapor−Liquid Equilibrium Results. The isothermal VLE data were experimentally determined via the HSGC method. In order to verify the reliability of the HSGC method used in this work, the isothermal VLE data of the citral (1) + linalool (2) system at 333.2 K were measured and the experimental data were compared with the literature data.[23] In Figure 2, the calculated AAPD was 0.85%, indicating that the HSGC method is reliable.

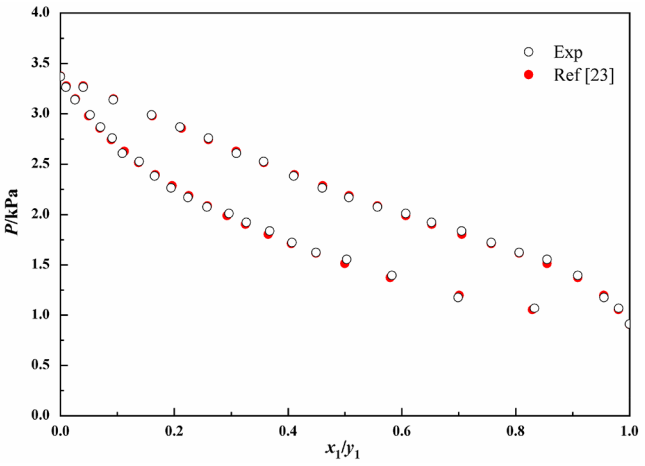

Figure 2. Comparison of experimental and literature data[23] for $P-x-y$ of the citral (1) + linalool (2) system at 333.2 K.

The isothermal VLE data of α-pinene (1), camphene (2), β-pinene (3), *p*-cymene (4), limonene (5), longifolene (6), and abietic acid + palustric acid + neoabietic acid + pimaric acid + sandopimaric acid + dehydroabietic acid + isopimaric acid (7) at 313.2 and 333.2 K are listed in Table 1. As shown, with an increasing mole fraction of the components of rosin, the mole fraction of the components of turpentine, such as α-pinene, camphene, β-pinene, *p*-cymene, and limonene in the liquid phase gradually decreased. However, the mole fraction of the less volatile component longifolene gradually increased. In contrast, in the vapor phase, the mole fraction of α-pinene increased while the other components showed a decreasing trend. Moreover, comparing the two temperatures, it was found that the higher the temperature was, the faster the mole fraction of each component increased or decreased. The isobaric data for α-pinene (1) + β-pinene (3),[14] α-pinene (1) + *p*-cymene (4),[15] α-pinene (1) + longifolene (6),[16] and α-pinene (1) + camphene (2)[17] have already been reported. However, the pressure and temperature range measured in this work were beyond that available in the literature. Thus, $x-y$ data comparisons with the literature and this work were not possible.

2.3. Activity Coefficients. The activity coefficient is related to the affinity between solutes and solvents, which is caused by differences in strength and properties between molecules. These differences were caused by local pairwise interactions of surface segments due to electrostatic dislocation, hydrogen bonding, and van der Waals dispersive forces.[24] The activity coefficients of α-pinene (1), camphene (2), β-pinene (3), *p*-cymene (4), limonene (5), and longifolene (6) of the turpentine + rosin system calculated using COSMO-RS at 313.2 and 333.2 K are presented in Table 2. As shown in Table 2, the activity coefficients decreased as the temperature increased. Moreover, when the mole fraction of

https://doi.org/10.1021/acsomega.1c05167
ACS Omega 2022, 7, 16270−16277

Table 1. VLE Data of α-Pinene (1), Camphene (2), β-Pinene (3), p-Cymene (4), Limonene (5), Longifolene (6), and Abietic Acid + Palustric Acid + Neoabietic Acid + Pimaric Acid + Sandopimaric Acid + Dehydroabietic Acid + Isopimaric Acid (7) Of Turpentine + Rosin System at 313.2 and 333.2 K[a]

x_7	x_1'	x_2'	x_3'	x_4'	x_5'	x_6'	y_1	y_2	y_3	y_4	y_5	y_6
						T/K = 313.2						
0.010	0.844	0.017	0.077	0.018	0.021	0.013	0.883	0.016	0.062	0.014	0.023	0.003
0.020	0.835	0.016	0.076	0.016	0.021	0.015	0.885	0.016	0.062	0.013	0.023	0.002
0.030	0.825	0.016	0.075	0.016	0.021	0.017	0.888	0.016	0.060	0.012	0.022	0.002
0.040	0.816	0.016	0.074	0.015	0.020	0.019	0.888	0.016	0.060	0.012	0.021	0.002
0.050	0.805	0.016	0.072	0.015	0.020	0.022	0.895	0.016	0.057	0.011	0.019	0.001
0.060	0.797	0.015	0.071	0.014	0.020	0.024	0.896	0.016	0.057	0.011	0.019	0.001
0.070	0.786	0.015	0.070	0.013	0.019	0.027	0.898	0.016	0.055	0.011	0.019	0.001
0.080	0.775	0.015	0.068	0.013	0.019	0.030	0.899	0.016	0.055	0.011	0.019	0.001
0.090	0.765	0.015	0.067	0.013	0.019	0.032	0.900	0.016	0.055	0.010	0.018	0.001
0.100	0.755	0.014	0.066	0.012	0.018	0.034	0.902	0.016	0.054	0.010	0.018	0.001
0.110	0.745	0.014	0.065	0.012	0.018	0.036	0.902	0.016	0.054	0.010	0.018	0.001
0.120	0.734	0.014	0.064	0.011	0.018	0.040	0.904	0.016	0.054	0.009	0.017	0.001
						T/K = 333.2						
0.010	0.843	0.017	0.077	0.016	0.021	0.016	0.892	0.014	0.058	0.014	0.020	0.002
0.020	0.834	0.016	0.076	0.016	0.021	0.018	0.894	0.014	0.058	0.013	0.019	0.002
0.030	0.824	0.016	0.075	0.015	0.021	0.019	0.898	0.014	0.058	0.010	0.018	0.002
0.040	0.815	0.016	0.073	0.015	0.020	0.020	0.899	0.014	0.057	0.010	0.018	0.001
0.050	0.805	0.016	0.073	0.015	0.020	0.022	0.899	0.014	0.057	0.010	0.018	0.001
0.060	0.793	0.016	0.072	0.015	0.020	0.026	0.901	0.014	0.057	0.010	0.018	0.001
0.070	0.783	0.015	0.069	0.013	0.019	0.032	0.900	0.014	0.056	0.010	0.018	0.001
0.080	0.773	0.015	0.068	0.013	0.019	0.033	0.901	0.014	0.056	0.010	0.018	0.001
0.090	0.764	0.014	0.067	0.012	0.019	0.034	0.902	0.014	0.056	0.010	0.018	0.001
0.100	0.754	0.014	0.067	0.012	0.019	0.036	0.902	0.014	0.056	0.010	0.017	0.001
0.110	0.745	0.014	0.065	0.011	0.018	0.037	0.903	0.014	0.056	0.010	0.017	0.001
0.120	0.734	0.014	0.064	0.011	0.018	0.041	0.905	0.014	0.055	0.009	0.017	0.001

[a]Standard uncertainties u are $u(T)$ = 0.1 K, $u(x_1)$ = 0.0021, and $u(y_1)$ = 0.0023.

the components of rosin increased, the activity coefficients of α-pinene, camphene, β-pinene, p-cymene, and limonene showed a gradually increasing trend but that of longifolene gradually decreased. It can also be seen from Table 2 that the activity coefficients were greater than 1 for all components of turpentine except for longifolene (6), indicating a positive deviation from Raoult's law for all components of turpentine except for longifolene, which is attributed to strong attractive forces in the liquid phase between the components of turpentine. It means that, under the conditions of a mixture of volatile components, for α-pinene, camphene, β-pinene, p-cymene, and limonene, the intermolecular forces of their mixture are less than those of the pure one, as described by Prausnitz et al.[25]

2.4. Total Pressure and Partial Pressure. The total pressure and partial pressure of α-pinene (1), camphene (2), β-pinene (3), p-cymene (4), limonene (5), and longifolene (6) of the turpentine + rosin system calculated using COSMO-RS are shown in Table 3. As shown in Table 3, the total and partial pressure were increased as the mole fraction of the rosin components and the temperature increased. The total pressure was about 1 kPa at 313.2 K and 3 kPa at 333.2 K. Moreover, α-pinene and β-pinene have the highest contribution to the total pressure since their molar fractions in the initial prepared samples were greater than those in the other components of turpentine.

2.5. Excess Gibbs Energies and Excess Enthalpies. The excess Gibbs energies G^E and excess enthalpies H^E of the system were calculated using COSMO-RS as shown in Table 4. As can be seen, G^E and H^E of the system were positive, indicating that the mixing process of the components of turpentine and rosin was endothermic. Moreover, both the G^E and H^E values increased with the decreasing mole fraction of turpentine components and increasing temperature. This may be attributed to the spatial effect. Since the components of rosin with a tricyclic phenanthrene skeleton are larger than the components of turpentine, with the mole fraction of the components of rosin increasing, the spatial effect makes the mixing of more rosin and the components of turpentine take more heat. Similar spatial effects are observed for mixtures of p-cymene + β-caryophyllene + 3-carene reported by Yao et al.[26]

As shown in Table 4, H^E(VDW) is negative, indicating that the interactions between homogeneous molecules are smaller than that between heterogeneous molecules. This is because of the heterogeneity between the components of turpentine and rosin, which is confirmed by the σ-profiles analysis. According to the distribution of σ-profiles in Figure 3, the surface shielding charges of the components of turpentine were distributed in the weak polar region of [−0.01,+0.01] e/Å^2, indicating that the components of turpentine were weakly polar molecules. Obviously, two broad peaks were observed in the [−0.02, − 0.01] e/Å^2 hydrogen bond donor region, which were attributed to hydroxyl oxygen for the components of rosin, while one broad peak in the hydrogen bond acceptor region of [+0.005, + 0.015] e/Å^2 was attributed to carbonyl, reflecting the fact that the components of rosin were the polar compounds with both hydrogen bond donors and hydrogen bond acceptors.

Moreover, as can be seen from Table 4, H^E(HB) contributes most to the excess enthalpies H^E, which is probably due to the

https://doi.org/10.1021/acsomega.1c05167
ACS Omega 2022, 7, 16270−16277

Table 2. Activity Coefficients of α-Pinene (1), Camphene (2), β-Pinene (3), p-Cymene (4), Limonene (5), and Longifolene (6) of the Turpentine + Rosin System at 313.2 and 333.2 K[a]

x_1'	γ_1	γ_2	γ_3	γ_4	γ_5	γ_6
			T/K = 313.2			
0.844	1.002	1.001	1.002	1.122	1.029	0.994
0.835	1.005	1.003	1.003	1.120	1.029	1.000
0.825	1.008	1.006	1.005	1.119	1.029	1.008
0.816	1.012	1.009	1.008	1.119	1.031	1.016
0.805	1.017	1.013	1.012	1.119	1.033	1.024
0.797	1.022	1.017	1.016	1.121	1.036	1.033
0.786	1.027	1.021	1.020	1.123	1.039	1.042
0.775	1.033	1.025	1.024	1.125	1.042	1.052
0.765	1.038	1.030	1.028	1.127	1.046	1.061
0.755	1.044	1.035	1.033	1.130	1.050	1.071
0.745	1.050	1.040	1.038	1.133	1.054	1.081
0.734	1.056	1.045	1.043	1.136	1.058	1.091
			T/K = 333.2			
0.843	1.001	1.001	1.002	1.110	1.026	0.991
0.834	1.003	1.002	1.002	1.106	1.025	0.997
0.824	1.006	1.004	1.004	1.104	1.025	1.003
0.815	1.009	1.006	1.006	1.103	1.025	1.009
0.805	1.013	1.009	1.008	1.102	1.026	1.016
0.793	1.017	1.012	1.011	1.103	1.028	1.024
0.783	1.021	1.015	1.014	1.104	1.030	1.032
0.773	1.025	1.019	1.017	1.105	1.032	1.040
0.764	1.030	1.022	1.021	1.106	1.035	1.048
0.754	1.035	1.026	1.025	1.107	1.038	1.056
0.745	1.040	1.030	1.028	1.109	1.041	1.065
0.734	1.044	1.035	1.032	1.111	1.044	1.074

[a]Standard uncertainties u, $u(\gamma_1)$ = 0.0051.

Table 3. Total Pressure and Partial Pressure of α-Pinene (1), Camphene (2), β-Pinene (3), p-Cymene (4), Limonene (5), and Longifolene (6) of the Turpentine + Rosin System at 313.2 and 333.2 K[a]

x_1'	P/kPa	P_1/kPa	P_2/kPa	P_3/kPa	P_4/kPa	P_5/kPa	P_6/kPa
			T/K = 313.2				
0.844	1.176	1.062	0.018	0.075	0.010	0.011	0.000
0.835	1.166	1.054	0.018	0.074	0.009	0.011	0.000
0.825	1.156	1.046	0.017	0.073	0.009	0.011	0.000
0.816	1.147	1.038	0.017	0.072	0.009	0.011	0.000
0.805	1.136	1.029	0.017	0.071	0.008	0.010	0.000
0.797	1.128	1.023	0.017	0.070	0.008	0.010	0.000
0.786	1.118	1.015	0.016	0.069	0.008	0.010	0.000
0.775	1.108	1.006	0.016	0.068	0.007	0.010	0.001
0.765	1.098	0.998	0.016	0.067	0.007	0.010	0.001
0.755	1.090	0.990	0.016	0.066	0.007	0.010	0.001
0.745	1.080	0.983	0.016	0.065	0.007	0.010	0.001
0.734	1.069	0.974	0.015	0.064	0.006	0.009	0.001
			T/K = 333.2				
0.843	3.206	2.888	0.049	0.208	0.027	0.033	0.001
0.834	3.176	2.863	0.048	0.205	0.027	0.032	0.001
0.824	3.145	2.837	0.047	0.202	0.026	0.032	0.001
0.815	3.120	2.816	0.047	0.200	0.025	0.031	0.001
0.805	3.092	2.790	0.046	0.198	0.025	0.031	0.001
0.793	3.056	2.758	0.046	0.196	0.024	0.031	0.002
0.783	3.020	2.733	0.044	0.189	0.022	0.031	0.002
0.773	2.996	2.712	0.043	0.187	0.021	0.030	0.002
0.764	2.972	2.691	0.043	0.186	0.021	0.030	0.002
0.754	2.946	2.668	0.043	0.184	0.020	0.029	0.002
0.745	2.922	2.649	0.042	0.180	0.019	0.029	0.002
0.734	2.890	2.622	0.041	0.177	0.019	0.029	0.003

[a]Standard uncertainties u, u(P)= 0.0089 kPa.

fact that the oxygen atom of the carboxyl group in the components of rosin can be considered as a hydrogen bond acceptor and can readily form hydrogen bonds with the methyl and methylene groups in the components of turpentine. This is consistent with the σ-profiles analysis results from Figure 3, where the peaks of +0.007 and +0.012 e/Å^2 are attributed to the oxygen atom of the carboxyl group in the components of rosin.

3. CONCLUSIONS

The isothermal VLE of the components of the turpentine + rosin system at 313.2 and 333.2 K were measured by headspace gas chromatography. The thermodynamic properties of the system such as activity coefficients, total pressure, partial pressure, excess Gibbs energies, and excess enthalpies were calculated using COSMO-RS model. The results showed that the activity coefficients were greater than 1 for all components of turpentine except for longifolene, indicating a positive deviation from Raoult's law. The total pressures were about 1 kPa at 313.2 K and 3 kPa at 333.2 K. Meanwhile, G^E and H^E of the system were positive, indicating that the mixing process for the components of turpentine and rosin was endothermic. The interactions between homogeneous molecules were smaller than those of heterogeneous molecules and resulted in negative H^E(VDW). Moreover, H^E(HB), which was caused by the hydrogen bonding interaction, contributed the most for the excess enthalpies H^E.

4. COMPUTATIONAL METHODOLOGY

4.1. COSMO-RS Model. The COSMO-RS (Conductor-like Screening Model for Realistic Solvation) model[27−34] allows prediction of thermodynamic properties of mixtures without relying on experimental data. The basis of the COSMO-RS model calculation is the surface shielding charge distribution σ. The intermolecular interaction can be described by the shielding charge interaction between the small pieces of molecules in contact with each other on the molecular surface. The energy of intermolecular interactions is given by eqs 2−4.[28]

$$E_{MF}(\sigma, \sigma') = a_{eff}\frac{\alpha'}{2}(\sigma, \sigma')^2 \quad (2)$$

$$E_{HB}(\sigma, \sigma') = c_{HB}\min(0, \sigma\sigma' + \sigma_{HB}^2) \quad (3)$$

$$E_{VDW}(\sigma, \sigma') = a_{eff}(\tau_{VDW} + \tau'_{VDW}) \quad (4)$$

where E_{MF} is the asymmetric energy of the shielding charge, E_{HB} is the energy of the intermolecular hydrogen bond, E_{VDW} is the energy of the reference state in solution, σ and σ' are the surface shielding charge density of the two interacting blobs, a_{eff} is the effective contact area, α' is an interaction parameter, c_{HB} is the hydrogen bond strength, σ_{HB} is the threshold for hydrogen bonding, and τ_{VDW} and τ'_{VDW} are element specific adjustable parameters.

The calculations using the COSMO-RS model occur over two steps. The first step is the quantum chemical calculations for the various substances involved in the system. These

https://doi.org/10.1021/acsomega.1c05167
ACS Omega 2022, 7, 16270−16277

Table 4. Excess Gibbs Energies and Excess Enthalpies of the Turpentine + Rosin System at 313.2 and 333.2 K

x_1'	H^E/ (J/mol)	H^E(MF)/ (J/mol)	H^E(HB)/ (J/mol)	H^E(VDW)/ (J/mol)	G^E/ (J/mol)
			T/K = 313.2		
0.844	139.687	66.868	73.230	−0.411	52.484
0.835	252.077	109.193	143.621	−0.736	91.372
0.825	344.371	144.623	200.509	−0.761	126.443
0.816	421.626	175.008	248.069	−1.451	158.291
0.805	500.745	201.564	300.718	−1.538	187.366
0.797	556.500	224.904	333.831	−2.234	213.990
0.786	607.553	245.866	364.592	−2.905	238.610
0.775	652.879	264.752	391.701	−3.574	261.415
0.765	693.206	281.775	415.676	−4.245	282.523
0.755	729.123	297.129	436.922	−4.928	302.054
0.745	761.294	311.069	455.805	−5.581	320.182
0.734	790.429	323.875	472.710	−6.156	337.130
			T/K = 333.2		
0.843	159.984	65.078	95.287	−0.381	45.268
0.834	273.442	109.734	164.436	−0.728	79.733
0.824	369.570	148.036	222.487	−0.953	111.133
0.815	442.107	181.450	262.219	−1.562	139.943
0.805	514.904	211.135	305.507	−1.738	166.544
0.793	578.999	237.748	343.631	−2.381	191.140
0.783	635.750	261.505	377.321	−3.075	213.783
0.773	686.354	283.000	407.221	−3.868	234.950
0.764	731.748	302.485	433.905	−4.641	254.621
0.754	772.651	320.216	457.812	−5.377	272.932
0.745	809.532	336.402	479.220	−6.090	290.010
0.734	843.303	351.370	498.625	−6.692	306.051

quantum chemical calculations for the COSMO-RS model are performed by the Turbomole software based on density generalization theory, which can generate cosmo files to describe the molecular surface shielding charge σ in a short time. The next step is the calculations of the microscopic intermolecular forces or the chemical potential to obtain thermodynamic properties by inputting the liquid phase composition and temperature using the COSMOtherm software.

4.2. Activity Coefficients. The activity coefficients for a given finite concentration can be calculated using the COSMO-RS model, in which the molar or mass fraction of the target compound is set as the desired value in the solvent composition. The activity coefficient of component i of the mixture at molar fraction x_i is calculated by eq 5.[35]

$$\ln(\gamma_i) = \frac{\mu_i^s(x) - \mu_i^{(p)}}{RT} \tag{5}$$

where $\mu_i^s(x)$ is the chemical potential of component i in the mixture, $\mu_i^{(p)}$ is the chemical potential of the pure component i, and R is the gas constant.

4.3. Pressure. The total pressure of the VLE is calculated by eq 6.

$$P = \sum_{i=1}^{n} P_i = \sum_{i=1}^{n} P_i^0 x_i \gamma_i \tag{6}$$

where P_i is the partial pressure of component i, P_i^0 is the vapor pressure of component i, x_i is the molar fraction of component i in the liquid phase, and γ_i is the activity coefficient of component i in the liquid phase. P_i^0 and γ_i are both calculated by the COSMOtherm software.

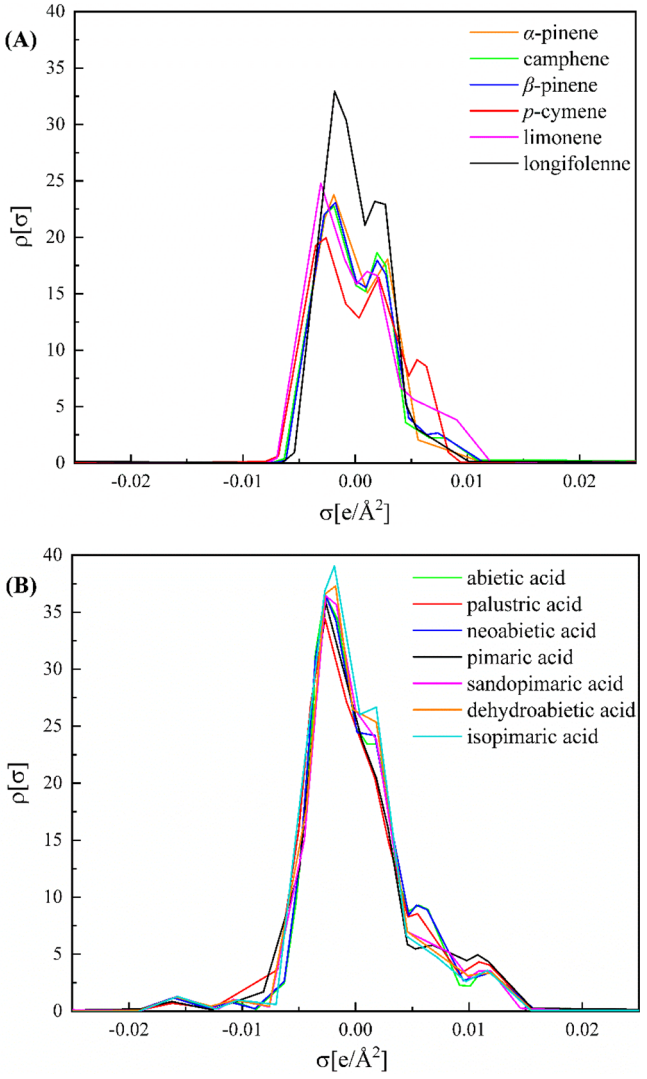

Figure 3. σ-Profiles of components of (A) turpentine and (B) rosin.

4.4. Excess Gibbs Energies. The excess Gibbs energies at a given temperature and mixing conditions are calculated by eq 7.

$$G^E = RT \sum_{i=1}^{n} x_i \ln(\gamma_i) \tag{7}$$

where x_i is the molar fraction of component i in the liquid phase, γ_i is the activity coefficient of component i in the liquid phase calculated by the COSMO-RS, and R is the gas constant.

4.5. Excess Enthalpies. To further investigate the nature of intermolecular interactions in solution, another important thermodynamic property, excess enthalpies H^E, is calculated by the COSMO-RS model based on eqs 8−11.

$$H^E = H^E(\mathrm{MF}) + H^E(\mathrm{HB}) + H^E(\mathrm{VDW}) \tag{8}$$

$$H^E(\mathrm{MF}) = x_1 H_1^E(\mathrm{MF}) + x_2 H_2^E(\mathrm{MF}) + \ldots + x_n H_n^E(\mathrm{MF}) \tag{9}$$

$$H^E(\mathrm{HB}) = x_1 H_1^E(\mathrm{HB}) + x_2 H_2^E(\mathrm{HB}) + \ldots + x_n H_n^E(\mathrm{HB}) \tag{10}$$

https://doi.org/10.1021/acsomega.1c05167
ACS Omega 2022, 7, 16270−16277

Table 5. Mole Fraction and CAS Numbers of the Main Components of Turpentine and Rosin Used in This Study

	components of turpentine					
	α-pinene	camphene	β-pinene	limonene	p-cymene	longifolene
mole fraction	0.851	0.017	0.078	0.018	0.022	0.014
CAS	80-56-8	79-92-5	127-91-3	138-86-3	99-87-6	475-20-7
	components of rosin					
	abietic acid	palustric acid	neoabietic acid	pimaric acid	dehydroabietic acid	sandopimaric acid	isopimaric acid
mole fraction	0.440	0.247	0.156	0.088	0.047	0.015	0.007
CAS	514-10-3	1945-53-5	471-77-2	127-27-5	471-74-9	1740-19-8	5835-26-7

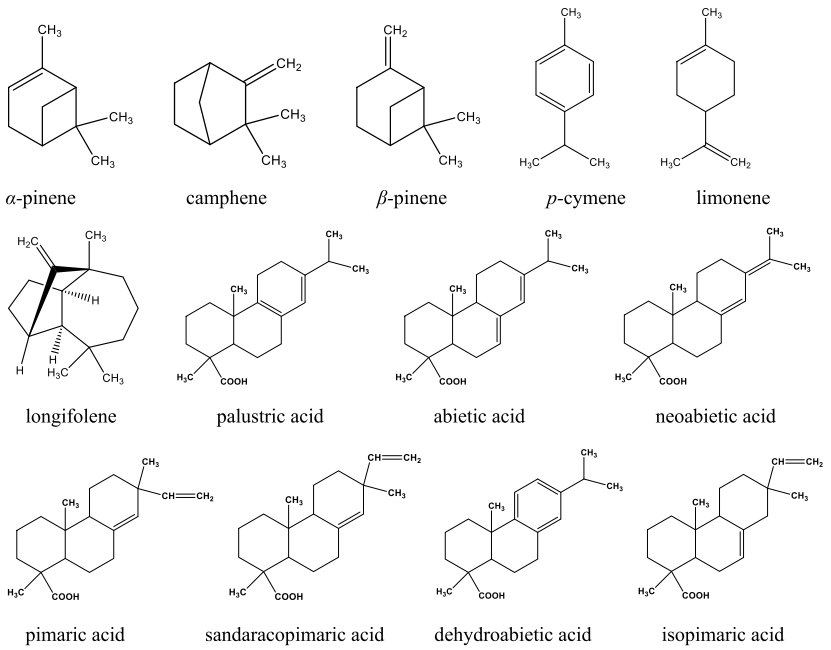

Figure 4. Molecular structures of the main components of turpentine and rosin used in this study.

$$H^{E}(\mathrm{VDW}) = x_1 H_1^{E}(\mathrm{VDW}) + x_2 H_2^{E}(\mathrm{VDW}) + \ldots + x_n H_n^{E}(\mathrm{VDW}) \quad (11)$$

where $H^{E}(\mathrm{MF})$ is the misfit interaction energy in the mixture, $H^{E}(\mathrm{HB})$ is the hydrogen bonding interaction energy in the mixture, $H^{E}(\mathrm{VDW})$ is the van der Waals interaction energy in the mixture, and H_i^{E} is computed as the expectation value of the partition sum of the microscopic segment−segment interaction enthalpies.[36] As shown in eq 8, the excess enthalpies H^{E} are composed of $H^{E}(\mathrm{MF})$, $H^{E}(\mathrm{HB})$, and $H^{E}(\mathrm{VDW})$.[37]

5. EXPERIMENTAL SECTION

5.1. Materials. Turpentine, provided by Guangxi Chaoyan Guoyou Forestry, mainly contains the following six components analyzed by gas chromatography: α-pinene, camphene, β-pinene, p-cymene, limonene, and longifolene. Rosin, provided by Guangxi Wuzhou Richeng Forestry Chemical Company, mainly contains the following seven components analyzed by gas chromatography: abietic acid, palustric acid, neoabietic acid, pimaric acid, dehydroabietic acid, sandopimaric acid, and isopimaric acid. The results of gas chromatography of turpentine and rosin are listed in Table 5. The molecular structures of the main components of turpentine and rosin are shown in Figure 4. Methanol (mass fraction, 99.9%, CAS, 67-56-1) and tetramethylammonium hydroxide solution (mass fraction, 25% aqueous solution, CAS, 75-59-2) were purchased from Shanghai Macklin Biochemical Company.

5.2. Apparatus and Procedure. The isothermal VLE data of components of the turpentine + rosin system at 313.2 and 333.2 K were measured by HSGC, which consists of a gas chromatography (GC) system (Agilent 7890B) and a headspace sampler (HS) (Agilent 7697A). GC included a HP-5 (30 m × 0.32 mm × 0.25 μm) capillary column and a flame ionization detector (FID), while HS included an electropneumatic sampling system and a precision thermostat with an accuracy of 0.1 K. The carrier gas of GC was N_2 (99.999%) with a constant flow rate of 25 mL/min. The column temperature was 323.2 K at the beginning, and ramped to 343.2 at 5 K/min, ramped to 403.2 at 10 K/min, then ramped to 483.2 at 5 K/min and finally 523.2 at 20 K/min. The injector and detector temperature were 523.2 K.

5.3. Sample Preparation. Samples were prepared in appropriate mass ratios using an analytical balance (Mettler Toledo) with a precision of 1×10^{-4} g. The rosin was first poured into the headspace vial (equilibrium cell, 20 mL), and the others were injected with a pipet gun. Then, the headspace vial was sealed with an aluminum cap and placed on a sample tray, followed by heating for 60 min in the thermostat. Since the sample mixture (approximately 5 mL) and equilibrium cell were too small, 60 min was sufficient for the vapor and liquid phase to equilibrate with each other. Finally, the vapor phase in the headspace vial was automatically sampled and transported

https://doi.org/10.1021/acsomega.1c05167
ACS Omega 2022, 7, 16270−16277

to the GC by the electro-pneumatic sampling system to obtain vapor phase composition. The liquid phase sample after vapor−liquid equilibrium was analyzed using GC following methyl esterification to obtain the liquid phase composition.

According to the properties and components of turpentine and rosin, six main components such as α-pinene (1), camphene (2), β-pinene (3), p-cymene (4), limonene (5), and longifolene (6) were selected for the VLE data measurements. The vapor−liquid phase components are all calculated by using eq 12.

$$x_i'/y_i = \frac{A_i/M_i}{\sum_{i=1}^{n} A_i/M_i} \quad (12)$$

where x_i' is the mole fraction of the six main components of turpentine in liquid phase without rosin, y_i is the mole fraction of the six main components of turpentine, A_i is peak area of component i in the vapor−liquid phase in gas chromatography, M_i is the molar mass of component i, and n is the six main components of turpentine.

AUTHOR INFORMATION

Corresponding Author

Jiezhen Liang − *Guangxi Key Laboratory of Petrochemical Resource Processing and Process Intensification Technology, School of Chemistry and Chemical Engineering, Guangxi University, Nanning 530004, China;* orcid.org/0000-0002-0032-7383; Phone: +86-771-3272702; Email: ljztony01@163.com; Fax: +86-771-323-3718

Authors

Youqi Li − *Guangxi Key Laboratory of Petrochemical Resource Processing and Process Intensification Technology, School of Chemistry and Chemical Engineering, Guangxi University, Nanning 530004, China;* orcid.org/0000-0002-0355-1321

Xiaopeng Chen − *Guangxi Key Laboratory of Petrochemical Resource Processing and Process Intensification Technology, School of Chemistry and Chemical Engineering, Guangxi University, Nanning 530004, China;* orcid.org/0000-0002-7496-3497

Linlin Wang − *Guangxi Key Laboratory of Petrochemical Resource Processing and Process Intensification Technology, School of Chemistry and Chemical Engineering, Guangxi University, Nanning 530004, China*

Xiaojie Wei − *Guangxi Key Laboratory of Petrochemical Resource Processing and Process Intensification Technology, School of Chemistry and Chemical Engineering, Guangxi University, Nanning 530004, China*

Minting Nong − *Guangxi Key Laboratory of Petrochemical Resource Processing and Process Intensification Technology, School of Chemistry and Chemical Engineering, Guangxi University, Nanning 530004, China*

Weijian Nong − *China Academy of Science and Technology Development Guangxi Branch, Nanning 530022, China; Guangxi Sci-Tech Development Forest-like Technology Co. LTD, Nanning 530022, China*

Complete contact information is available at: https://pubs.acs.org/10.1021/acsomega.1c05167

Notes

The authors declare no competing financial interest.

ACKNOWLEDGMENTS

We acknowledge the financial support for this work from the National Natural Science Foundation of China (No. 31960294, 32160349), Guangxi Key Laboratory of Petrochemical Resource Processing and Process Intensification Technology (No. 2017Z005, 2020Z005), and the Project for Cultivating New Century Academic and Technology Leaders of Nanning City (No. 2020010).

REFERENCES

(1) García-Navas, D. F.; Bustamante, F.; Villa, A. L.; Alarcón, E. Esterification of rosin with methyl alcohol for fuel applications. *Rev. Fac. Ing. Univ. Antioquia* **2020**, *100*, 10−20.

(2) Liu, P.; Liu, X. M.; Saburi, T.; Kubota, S.; Huang, P. X.; Wada, Y. Thermal Stability Evaluation of Resin Acids and Rosin Modified Resins. *ACS omega.* **2020**, *5* (45), 29102−29109.

(3) Han, C. R.; Zhou, R. N.; Han, B.; Tian, C.; Xu, P. F.; Song, X. L. The research progress in molecular self-assembly of rosin resin acids and their derivatives. *Chem. Ind. For. Prod.* **2019**, *39* (5), 1−10.

(4) Yu, C.; Chen, C. W.; Gong, Q. H.; Zhang, F. A. Preparation of polymer microspheres with a rosin moiety from rosin ester, styrene and divinylbenzene. *Polym. Int.* **2012**, *61* (11), 1619−1626.

(5) Tao, P.; Li, J. J.; Li, J.; Shang, S. B.; Song, Z. Q. Enhanced performance of rosin-based epoxy composites mixed with carbon nanotubes and cork powders from oriental oak bark. *Ind. Crops. Prod.* **2020**, *158*, 113051.

(6) Li, Q. G.; Liu, H.; Shang, S. B.; Song, Z. Research progress of rosin and its derivatives in polymer synthesis. *Chem. Ind. For. Prod.* **2017**, *37* (4), 23−29.

(7) Vevere, L.; Fridrihsone, A.; Kirpluks, M.; Cabulis, U. A Review of Wood Biomass-Based Fatty Acids and Rosin Acids Use in Polymeric Materials. *Polymers.* **2020**, *12* (11), 2706.

(8) Kugler, S.; Ossowicz, P.; Malarczyk-Matusiak, K.; Wierzbicka, E. Advances in rosin-based chemicals: the latest recipes, applications and future trends. *Molecules* **2019**, *24* (9), 1651.

(9) Jeevanantham, A. K.; Reddy, D. M.; Goyal, N.; Bansal, D.; Kumar, G.; Kumar, A.; Nanthagopal, K.; Ashok, B. Experimental study on the effect of cetane improver with turpentine oil on CI engine characteristics. *Fuel* **2020**, *262*, 116551.

(10) Farcas, A. D.; Mot, A. C.; Zagrean-Tuza, C.; Ticolea, M.; Sevastre, B.; Kulak, M.; Silaghi-Dumitrescu, R.; Parvu, A. Remarkable rutin-rich Hypericum capitatum extract exhibits anti-inflammatory effects on turpentine oil-induced inflammation in rats. *BMC Complementary Altern. Med.* **2019**, *19* (1), 1−13.

(11) Kaplan, C.; Alma, M. H.; Tutus, A.; Çetinkaya, M.; Karaosmanoğlu, F. Engine performance and exhaust emission tests of sulfate turpentine and No: 2 diesel fuel blend. *Pet. Sci. Technol.* **2005**, *23* (11−12), 1333−1339.

(12) Zhang, Q. G.; Bi, L. W.; Zhao, Z. D.; Chen, Y. P.; Li, D. M.; Gu, Y.; Wang, J.; Chen, Y. X.; Bo, C. Y.; Liu, X. Z. Application of ultrasonic spraying in preparation of p-cymene by industrial dipentene dehydrogenation. *Chem. Eng. J.* **2010**, *159*, 190−194.

(13) Cătunescu, G. M.; Socaci, S. A.; Rotar, I.; Vidican, R.; Bunghez, F.; Tofană, M.; Plesa, A.; Muntean, M. Volatile profile of minimally processed herbs during cold storage. *Rom. Biotechnol. Lett.* **2016**, *21* (5), 11923.

(14) Wang, L. L.; Chen, X. P.; Wei, X. J.; Ma, J. Study on the vapor−liquid equilibrium of α-pinene and β-pinene system. *Nat. Gas. Ind.* **2002**, *3*, 57−60 (in Chinese).

(15) Sun, L. X.; Liao, D. Q.; Wang, K.; Sun, J. H.; Tong, Z. F. Vapor-liquid equilibrium data for α-pinene + β-pinene + p-cymene at reduced pressure. *J. Chem. Ind. Eng.* **2018**, *69* (7), 2822−2828 (in Chinese).

(16) Ruan, F. X.; Che, J. J.; Hu, J.; Wang, Y.; Yuan, Bo.; Zhou, L. C. Vapor−liquid equilibrium of pinnae−α-pinene−longifolene system and its excess Gibbs free energy and excess enthalpy. *J. Chem. Eng. Chin. Univ.* **2015**, *29* (6), 1306−1312 (in Chinese).

(17) Wu, J. Z.; Wang, L. L.; Chen, X. P.; Wei, X. J.; Liang, J. Z.; Yao, G. Y.; Zheng, P. Measurement and correlation of vapor−liquid equilibrium data for binary systems composed of camphene, (+)-3-carene, (−)-β-caryophyllene, *p*-cymene, and α-pinene at 101.33 kPa. *Thermochim. Acta* **2019**, *679*, 178318.
(18) Kolb, B.; Ettre, L. S. *Static headspace-gas chromatography: theory and practice*; John Wiley & Sons, 2006.
(19) Dai, Y.; Yu, Z. H.; Zhan, J. B.; Yue, B. S.; Xie, J.; Wang, H.; Chai, X. S. Determination of starch gelatinization temperatures by an automated headspace gas chromatography. *J. Chromatogr. A* **2019**, *1602*, 419−424.
(20) Yan, N.; Wan, X. F.; Chai, X. S.; Chen, R. Q. Determination of Chlorinated Volatile Organic Compounds in Polyamine Epichlorohydrin Solution by Headspace Gas Chromatography. *J. Chromatogr. A* **2017**, *1496*, 163−166.
(21) Wichitnithad, W.; Sudtanon, O.; Srisunak, P.; Cheewatanakornkool, K.; Nantaphol, S.; Rojsitthisak, P. Development of a Sensitive Headspace Gas Chromatography−Mass Spectrometry Method for the Simultaneous Determination of Nitrosamines in Losartan Active Pharmaceutical Ingredients. *ACS omega.* **2021**, *6* (16), 11048−11058.
(22) Xu, X. Q.; Liao, D. Q.; Li, L. S.; Chen, X. P.; Tong, Z. F. Determination and correlation of atmospheric pressure vapor−liquid equilibrium of α-alkene + β-pinene + *p*-cymene hydrocarbons. *J. Chem. Eng.* **2007**, 2970−2974 (in Chinese).
(23) Zheng, P.; Wang, L. L.; Chen, X. P.; Wei, X. Z.; Liang, J. Z.; Wu, J. Z. Excess Gibbs Energies and Isothermal Vapor−Liquid Equilibrium for Citral + Linalool, Citral + α-Pinene, and Linalool + α-Pinene Systems Using Headspace Gas Chromatography. *J. Chem. Eng. Data* **2020**, *65* (7), 3593−3604.
(24) Chu, Y. H.; Zhang, X. P.; Hillestad, M.; He, X. Z. Computational prediction of cellulose solubilities in ionic liquids based on COSMO-RS. *Fluid Phase Equilib.* **2018**, *475*, 25−36.
(25) Prausnitz, J. M.; Lichtenthaler, R. N.; De Azevedo, E. G. *Molecular thermodynamics of fluid-phase equilibria*; Pearson Education. 1998.
(26) Yao, G. Y.; Wang, L. L.; Chen, X. P.; Liao, D. Q.; Tong, Z. F.; Lei, F. H.; Li, P. F. Excess enthalpies of binary systems of β-strophanthrene, *p*-cymene and 3-carene. *J. Chem. Eng. Chin. Univ.* **2018**, *32* (4), 779−784 (in Chinese).
(27) Klamt, A. Conductor-like screening model for real solvent: a new approach to the quantitative calculation of solvation phenomena. *J. Phys. Chem.* **1995**, *99* (7), 2224−2235.
(28) Klamt, A.; Eckert, F. COSMO-RS: a novel and efficient method for the priori prediction thermo-physical data of liquids. *Fluid Phase Equilib.* **2000**, *172* (1), 43−72.
(29) Klamt, A.; Krooshof, G. J. P.; Taylor, R. COSMOSPACE: alternative to conventional activity coefficient models. *AIChE J.* **2002**, *48* (10), 2332−2349.
(30) Klamt, A. The COSMO and COSMO-RS solvation models. *Wiley Interdiscip. Rev.: Comput. Mol. Sci.* **2011**, *1* (5), 699−709.
(31) Sinnecker, S.; Rajendran, A.; Klamt, A.; Diedenhofen, M.; Neese, F. Calculation of solvent shifts on electronic g-tensors with the conductor-like screening model (COSMO) and its self-consistent generalization to real solvents (direct COSMO-RS). *J. Phys. Chem. A* **2006**, *110* (6), 2235−2245.
(32) Klamt, A.; Eckert, F. Prediction of vapor liquid equilibria using COSMOtherm. *Fluid Phase Equilib.* **2004**, *217* (1), 53−57.
(33) Gaudin, T. Exploring direct prediction of surface tension from COSMO-RS theory. *Chem. Phys. Lett.* **2018**, *706*, 308−31.
(34) Loschen, C.; Reinisch, J.; Klamt, A. COSMO-RS based predictions for the SAMPL6 logP challenge. *J. Comput. Aided Mol. Des.* **2020**, *34* (4), 385−392.
(35) Balchandani, S.; Singh, R. COSMO-RS Analysis of CO_2 Solubility in N-Methyldiethanolamine, Sulfolane, and 1-Butyl-3-methyl-imidazo- lium Acetate Activated by 2-Methylpiperazine for Postcombustion Carbon Capture. *ACS omega.* **2021**, *6* (1), 747−761.
(36) Ruiz, E.; Ferro, V. R.; Palomar, J.; Ortega, J.; Rodriguez, J. J. Interactions of ionic liquids and acetone: thermodynamic properties, quantum-chemical calculations, and NMR analysis. *J. Phys. Chem. B* **2013**, *117* (24), 7388−7398.
(37) Wang, Z. H.; Liu, S. L.; Jiang, Y. F.; Lei, Z. G.; Zhang, J.; Zhu, R. S.; Ren, J. W. Methyl chloride dehydration with ionic liquid based on COSMO-RS model. *Green Energy Environ.* **2021**, *6* (3), 413−421.

https://doi.org/10.1021/acsomega.1c05167
ACS Omega 2022, 7, 16270−16277